

## **Investigation of CO<sub>2</sub> Corrosion Inhibitor Adsorption and Desorption Behavior Using Langmuir Isotherm Model and Effects of Iron Carbide on CI Persistency**

Kasra Shayar Bahadori, Bruce Brown, Marc Singer  
Institute for Corrosion and Multiphase Technology  
Department of Chemical and Biomolecular Engineering  
Ohio University  
334 W State St  
Athens, OH, 45701  
USA

### **ABSTRACT**

One of the most conventional methods to mitigate CO<sub>2</sub> corrosion of pipelines in the oil and gas industry is to use chemical corrosion inhibitors. Probably the most commonly used inhibition method in the upstream oil and gas industry involves the continuous injection of an appropriate chemical formulation package to maintain a constant concentration of inhibitor in the fluid flowing through the pipeline. Selection of the inhibitor package is typically done through a tedious laboratory testing campaign, which involves the determination of the inhibitor efficiency and persistency in simulated production conditions. Developing laboratory methodologies that can help assessing these properties is of prime importance. This study presents methodologies that could simulate continuous inhibitor treatment (for the determination of efficiency), and also interruption of inhibitor injection (for the assessment of persistency). The study was performed using a model, yet representative, compound benzyldimethylammonium type CO<sub>2</sub> corrosion inhibitor (BDA-C14). Its adsorption/desorption behavior was characterized. Furthermore, the influence of several key aspects of the experimental methodologies, such inhibitor contact and pre-corrosion times were examined using BDA-C14, mostly to investigate the effects of the iron carbide layer on inhibitor persistency. A three-electrode system using a rotating cylinder electrode (RCE) for the working electrode was used in this study with the ability for continuous flow-through dilution. All experiments were divided into three main steps: pre-corrosion, inhibitor addition and corrosion rate stabilization, then inhibitor dilution. The corrosion rate was monitored using linear polarization resistance (LPR) in all experiments. Langmuir isotherm model was used to model inhibitor adsorption and desorption behavior of BDA-C14 inhibitor using calculated kinetic coefficients.

**Keywords:** CO<sub>2</sub> corrosion, corrosion inhibition, inhibitor persistency, continuous treatment, adsorption and desorption, Langmuir model

## INTRODUCTION

CO<sub>2</sub> corrosion of the internal walls of mild steel pipelines has always been a significant problem in the oil and gas industries. Different methods have been implemented to mitigate internal pipeline corrosion. The use of corrosion inhibitors provides advantages compared to other mitigation techniques as inhibitor treatment costs are seen to be lower and can be easily adjusted over time. Thus, chemical inhibitors are widely used as a conventional method to mitigate internal pipeline corrosion. Inhibitors are injected inside producing pipelines using two main methods : continuous corrosion inhibitor (CI) injection and batch inhibitor (BI) treatment.<sup>1-7</sup> In continuous CI treatment (which is of interest in this study), water-soluble inhibitor solutions are injected into the flow stream at a specific volumetric flow rate to obtain the desired concentration, which is typically below 2000 ppm(v). These inhibitors are not expected to form a tenacious film on the pipeline inner surface. The properties on the inhibitor film present on the metal surface are controlled by the inhibitor bulk concentration and the adsorption/desorption equilibrium. Therefore, if an interruption to the continuous injection occurs, the bulk inhibitor concentration in the flow stream decreases rapidly and the inhibitor is expected to desorb from the surface, resulting in a loss of corrosion protection. Adsorption and desorption behaviors of inhibitor molecules depend on several parameters: the physicochemical characteristics of the CI, characteristics of the metal surface, and flow stream conditions (temperature and flow rate).<sup>2-12</sup>

The corrosion inhibitors behavior in continuous treatment is often evaluated in laboratory conditions prior to field application. Different studies have developed experimental procedures to simulate both continuous and batch treatment.<sup>8, 13-16</sup> However, there have always been some difficulties in getting reproducible results due to the lack of consistency and clarity in testing protocols. Nevertheless, a common acceptable experimental procedure for mimicking the 'failure' of a continuous treatment program in the laboratory could be found in the literature:<sup>8, 13-16</sup>

1. Prepare deoxygenated solution and metal specimen for a glass cell setup.
2. Measure blank corrosion rate (CR) in a CO<sub>2</sub> saturated solution under specific test conditions without inhibitor (pre-corrosion step).
3. Inject a targeted concentration of inhibitor and measure the stable inhibited corrosion rate (inhibition step) after some time period.
4. Flush the inhibited solution from the glass cell and replace it with an uninhibited solution or move the working electrode from an inhibited electrolyte to an identical uninhibited environment (dilution step).
5. Measure the corrosion rate over time until it increases back to the blank corrosion rate (CR) to determine CI persistency.

The most important step in the simulated experiment of continuous treatment is the "dilution" step, which should reproduce the sudden decrease in the bulk CI concentration. However, limited studies have been conducted using a procedure that effectively continuously decreases the bulk concentration of the inhibitor to undetectable level.

Correlations between corrosion inhibition and adsorption/desorption behaviors are typically developed using isotherm models. Several isotherm models can be found in the literature. The most common ones, that are used for interaction between inhibitor molecules and the metal surface, are the Langmuir, Frumkin, Bockris-Swinkels and Virial Parson isotherms. Among these isotherms, the Langmuir isotherm model is the simplest and most widely used in the literature. This model assumes that molecules adsorb on the surface by forming a monolayer and the interaction between the adsorbate molecules is negligible.

In this study, a Langmuir isotherm model was used to calculate the adsorption/desorption kinetics followed by modeling the corrosion rate in both the inhibition and dilution steps .<sup>17-22</sup>

## EXPERIMENTAL PROCEDURE

### Experimental procedure for simulation of (interruption in) continuous treatment

The system set-up described below was used to investigate the effect of continuous dilution of the inhibited solution on inhibitor persistency. All experiments were done in a 3-electrode glass cell apparatus (Figure 1). Experiments investigating the persistency of the inhibitor including the continuous dilution step were performed using an overall larger setup shown in Figure 2. The test matrix for experimental procedures is shown in Table 1.

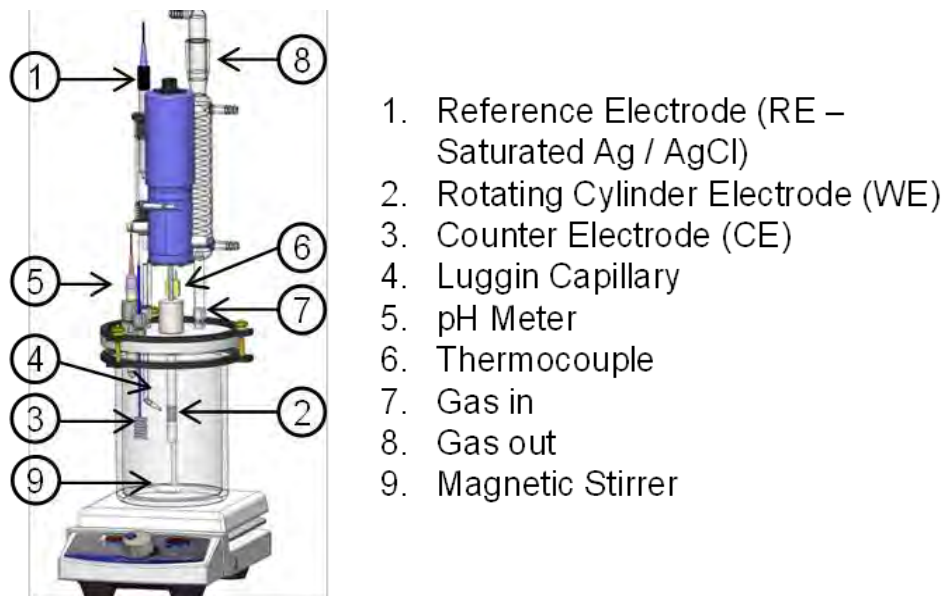
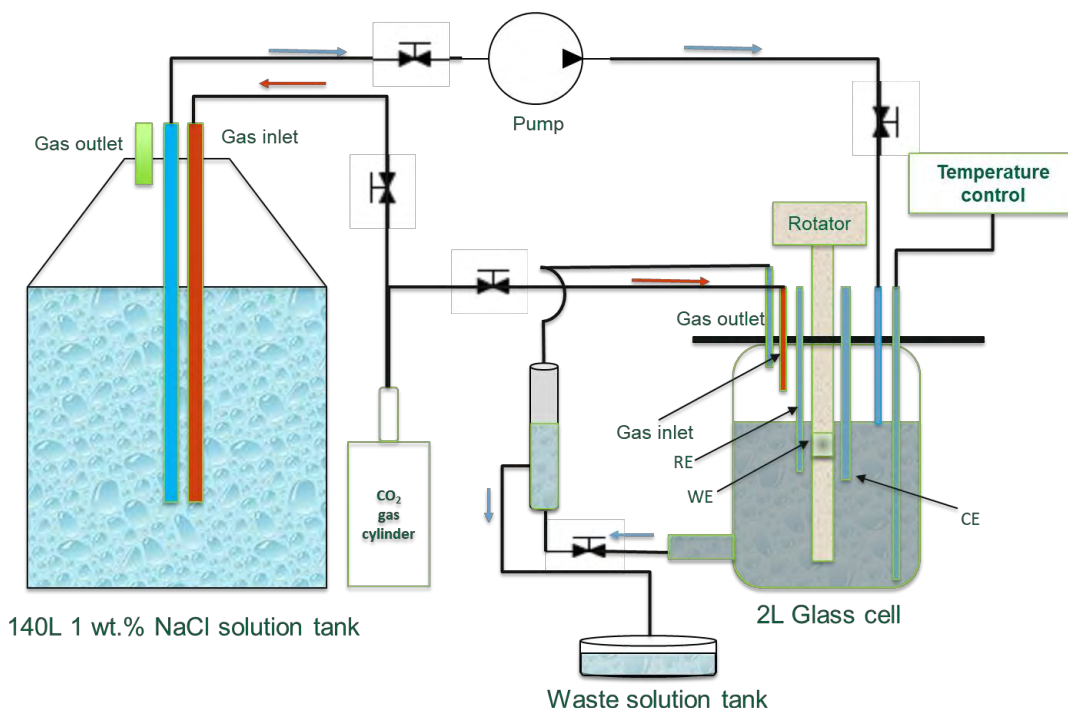


Figure 1: 3-electrode glass cell setup



**Figure 2: Schematic of the setup used in persistency experiments which provided continuous dilution.**

**Table 1  
Experimental test matrix for the continuous treatment experiments**

Parameter	Conditions
Working electrode	API 5L X65 (0.05 wt.%C)
Electrolyte	1 wt.% NaCl
Sparge gas	CO <sub>2</sub>
Total pressure	1 bar
Rotational speed	1000 RPM
Temperature	30°C ± 1°C
pH	4.0 ± 0.1
Corrosion inhibitor (CI) model compound	Quaternary ammonium type (BDA-C14)
Measurement methods	OCP, LPR, EIS
Initial inhibitor concentration	50 ppm
Presence of hydrocarbon	None – brine only
Pre-corrosion before CI injection	20 minutes and 2 hours
Contact time with the inhibitor (time before dilution)	9 hours and 29 hours
CI measurement method	UV-vis spectroscopy

The general procedure for experiments simulating continuous dilution of the inhibitor is as follows:

1. Fill the system and glass-cell with electrolyte (1 wt.% NaCl).
2. Sparge complete system with CO<sub>2</sub> for a minimum of 1 hour to keep the dissolved O<sub>2</sub> content to a few ppb.

3. Insert polished steel specimen in glass cell and complete pre-corrosion LPR measurements for 10 min.
4. Inject corrosion inhibitor, continue LPR measurements.
5. After a stable inhibited corrosion rate is obtained, dilution is started by pumping fresh brine (deoxygenated and sparged with CO<sub>2</sub> at the same working temperature) to the working glass cell. An overflow technique is used to continuously drain the solution at the same rate as solution is added while keeping liquid level constant and not allowing oxygen to backflow into the working glass cell.
6. LPR measurements are continued at 30-minute intervals until a new stable corrosion rate is obtained.
7. Periodic sampling of the solution was done to confirm the decrease of inhibitor concentration, by taking 10 mL of the solution from the outlet each time.

The following sections provide more details on different steps of the procedures.

#### Pre-corrosion

1.8 L of 1 wt.% NaCl was purged in a three-electrode glass cell for an hour to ensure deoxygenation and facilitate CO<sub>2</sub> saturation. The concentration of the oxygen was monitored during the experiment via an Orbisphere<sup>†</sup> 410 connected to the gas outlet of the system. The working electrode then was carefully mounted on the rotating shaft after polishing to a 600-grit finish. The open circuit potential was monitored for 10 minutes for a stable value and then LPR was measured prior to inhibitor injection.

#### Inhibitor preparation and delivery

136 mg solid BDA-C14 was weighed in a vial which was previously cleaned using isopropanol in an ultra-sonic cleaner. 3 ml isopropanol was injected into the vial containing solid inhibitor and then was fully mixed using the same ultra-sonic device for 20 minutes. 2 ml of this mixed solution was injected into the main solution (1.8L 1 wt.% NaCl) using a long needle into the bulk solution to attain 50 ppm<sub>w</sub> concentration of the inhibitor.

#### Dilution procedure

The dilution step was performed by equalizing input and output flowrate using an overflow technique to transfer brine from a 140 L supply at a rate of approximately 80±10 mL/min. This would “fully exchange” the solution in the glass cell every 22 minutes. The fluid renewal was continued until the end of the test. This method should remove all the inhibitor residuals from the solution, which is a key factor in simulating field condition in continuous treatment. With this dilution method, the change in bulk inhibitor concentration with regards to time can be calculated as follows:

$$C_{inh}(t) = C_{inhibitor_0} e^{-\frac{Q}{V}t} \quad (1)$$

where  $C_{inhibitor_0}$ ,  $Q$ ,  $V$ , and  $t$  are initial inhibitor concentration (ppm), dilution flowrate (L/min), solution volume (L), and time after dilution (min) respectively.

#### CI concentration measurement using UV-vis spectroscopy

The initial and residual inhibitor concentrations were measured during the experiments. Liquid samples were taken directly from the working glass cell at different times of the experiment and their absorbance

---

<sup>†</sup> Trade name.

was measured using an Agilent Cary 60<sup>‡</sup> UV-Vis spectrophotometer. The calibration curve was made from pre-mixed known solutions containing BDA-C14 in a 1 wt% NaCl solution and plotting the measured absorbance vs. concentration according to Beer's law, Equation (2). This technique is not valid for every corrosion inhibitor as it requires that the inhibitor displays structural moieties that can be detected *via* UV-Vis spectroscopy.

$$A = \epsilon l C \quad (2)$$

$A$  = Absorbance measured with UV-Vis spectroscopy

$\epsilon$  = Absorption coefficient ( $M^{-1} \cdot cm^{-1}$ )

$C$  = Concentration ( $M^{-1}$ )

$l$  = Path length ( $cm$ )

The UV-vis calibration curve for BDA-C14 is shown in Figure 3. Using this calibration data, an equation for determining the inhibitor concentration in the liquid samples taken during the experiments is shown as Equation (3):

$$CI \text{ concentration (ppm)} = \frac{\text{Absorbance}}{0.0279} \quad (3)$$

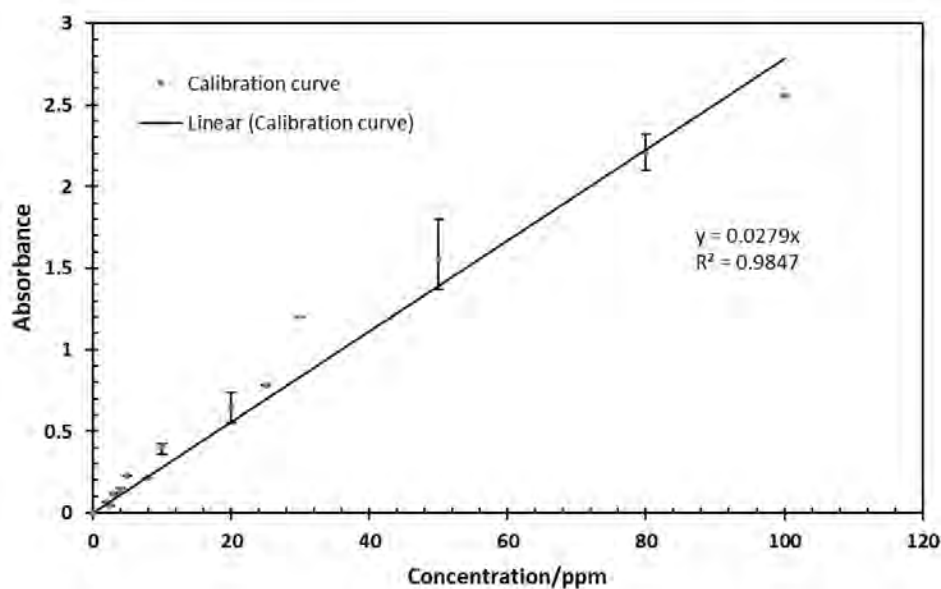


**Figure 3: BDA-C14 UV-vis calibration curve.**

<sup>‡</sup> Trade name

© 2023 Association for Materials Protection and Performance (AMPP). All rights reserved. No part of this publication may be reproduced, stored in a retrieval system, or transmitted, in any form or by any means (electronic, mechanical, photocopying, recording, or otherwise) without the prior written permission of AMPP.

Positions and opinions advanced in this work are those of the author(s) and not necessarily those of AMPP. Responsibility for the content of the work lies solely with the author(s).

Figure 4 Shows the structure of benzyldimethylammonium (BDA-C14) with 14 carbons as the tail group used in this study. The surface saturation concentration for this inhibitor is measured in previous study as 20 ppm<sub>w</sub>.<sup>8</sup>

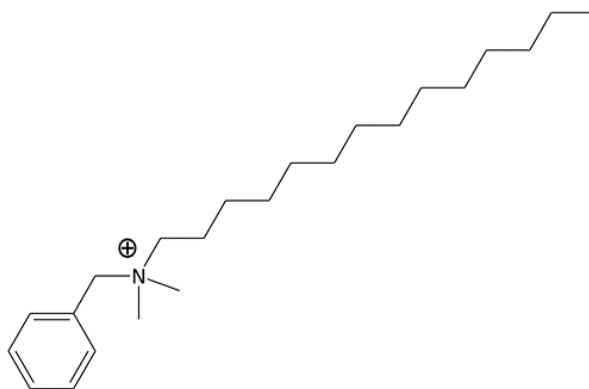


**Figure 4: Structure of quaternary ammonium inhibitor (BDA-C14).**

## RESULTS AND DISCUSSION

### Experimental results

#### Persistency at 30°C with 20 minutes pre-corrosion and 9 hours contact time:

Three repeat experiments were done at 30°C to investigate the behavior of the inhibitor adsorption/desorption with 20 minutes of pre-corrosion. Figure 5 shows the results for three attempts which demonstrates good reproducibility of the experiments. The average corrosion rate before addition of the inhibitor was 3.7±0.5 mm/year which reduced to 0.15±0.05 mm/year 9 hours after the inhibitor injection (95.9% efficiency). After the dilution step began, the corrosion rate remained stable for 1.5 hours. Results suggest that the reason for this behavior was due to the complete removal of inhibitor from the main glass cell. In other words, the corrosion rate did not increase until all the inhibitor residuals were removed from the glass cell by the continuous dilution.

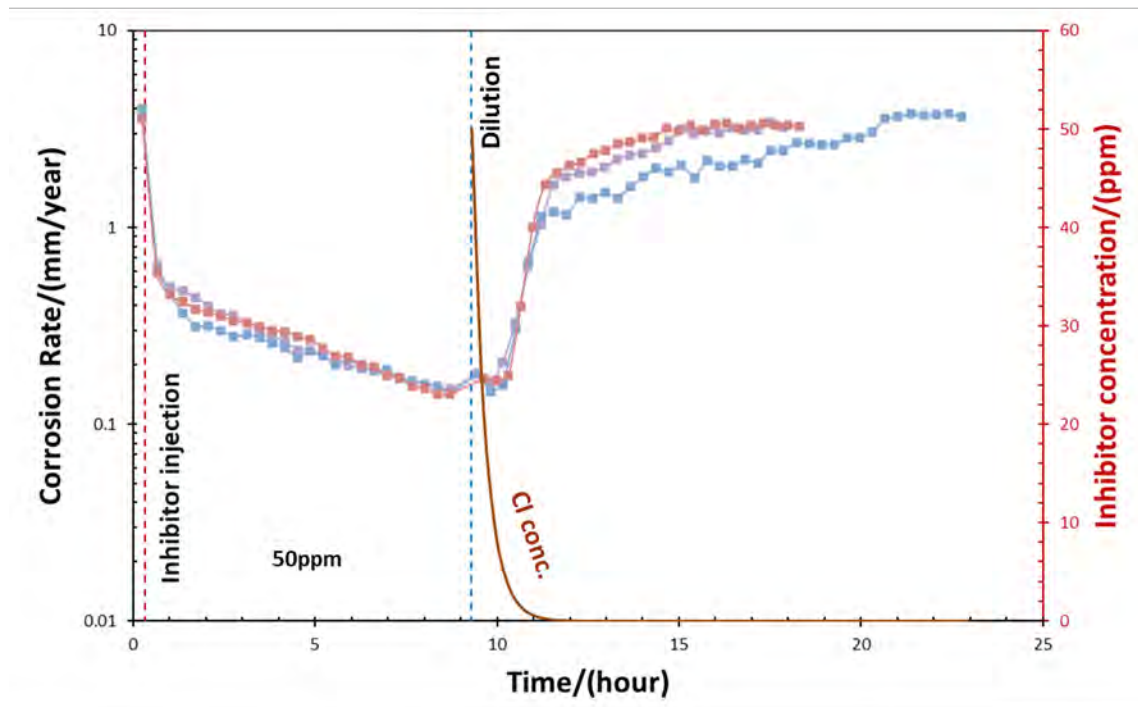


**Figure 5: Corrosion rate and Cl concentration versus time for 20 minutes pre-corrosion and three different repeats (30°C, 0.97 bar pCO<sub>2</sub>, X65 RCE, 1000 rpm, BDA-C14 inhibitor, 9 hours contact time).**

Results in Figure 5 clearly show that complete removal of the inhibitor, through constant dilution, resulted in full desorption of the inhibitor and little to no persistency of BDA-C14.

Persistency at 30°C with longer contact time and 20 minutes pre-corrosion:

Two repeat experiments were done to investigate the effects of a longer contact time of the RCE with the inhibitor in solution. Note the inhibited corrosion rates at ~10 hours were 0.15 and 0.05 mm/yr (similar to Figure 5) but continued to decrease to 0.085 and 0.04 mm/yr, respectively, in Figure 6 (~98.4% efficiency). In both cases, the corrosion rate increased right after the dilution began. However, neither test returned to the initial corrosion rate, even after 30 to 65 hours of the dilution. After 1<sup>st</sup> hour of dilution, the slope of corrosion rate vs. time decreased dramatically, leading to a slow, almost continuous, loss of mitigation over time until the end of each test. The stable corrosion rate observed during this dilution step, after 65 hours of exposure, was well below the uninhibited value and was also still lower than the experiments with 9 hours of contact time.

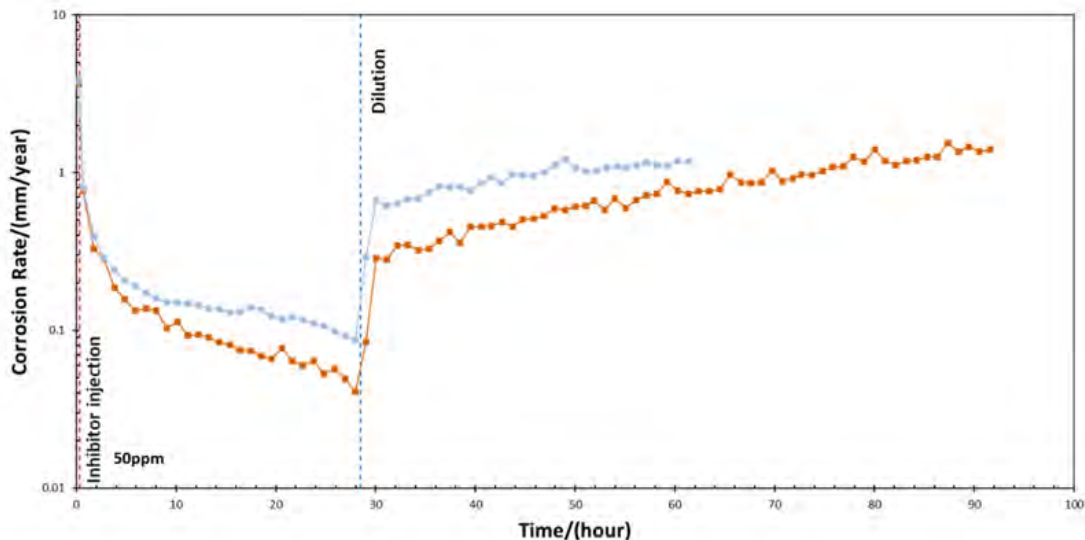


**Figure 6: Corrosion rate versus time for longer contact time of 29 hours and two different repeats (30°C, 0.97 bar pCO<sub>2</sub>, X65 RCE, 1000 rpm, BDA-C14 inhibitor, 20 minutes pre-corrosion).**

In each test above, the working electrode was removed, polished, and put back to the same solution to measure corrosion rate to verify if any residual inhibitor was remaining in the glass cell. For each test, this corrosion rate was similar to the initial corrosion rate in uninhibited solution which confirmed the effective removal of all inhibitor molecules from the glass cell. This suggests that the increase in contact time, from 9 to 28 hours, lead to slightly slower desorption kinetics of the inhibitor. Even though the corrosion rate was low, it is assumed that the slight change in surface roughness, and the presence of a thin iron carbide layer on the metal surface altered the surface characteristics and the inhibitor desorption kinetics.

Persistency at 30°C with 2 hours pre-corrosion and 9 hours contact time:

Another set of experiments was done to clarify the effects of initial pre-corrosion, or iron carbide layer development, on inhibitor desorption behavior and its persistency. Figure 7 shows two different experiments with 2 hours pre-corrosion and 9 hours of contact time. The initial corrosion rates before inhibitor injection were  $3.7 \pm 0.5$  mm/yr with inhibited rates of  $0.05 \pm 0.01$  mm/yr after 9 hours (98.6% efficiency). As compared to Figure 5, results clearly show that the desorption kinetics of the BDA-C14 were influenced by the increasing pre-corrosion time, which is thought to be related to having more iron carbide exposed on the metal surface. A slight increase in corrosion rate was observed when dilution was started, and about 1 hour of inhibitor persistency was seen before the corrosion rate begins to increase. Compared to Figure 5 (with 20 minutes pre-corrosion), 2-hours pre-corrosion led to a slower and incomplete inhibitor desorption.

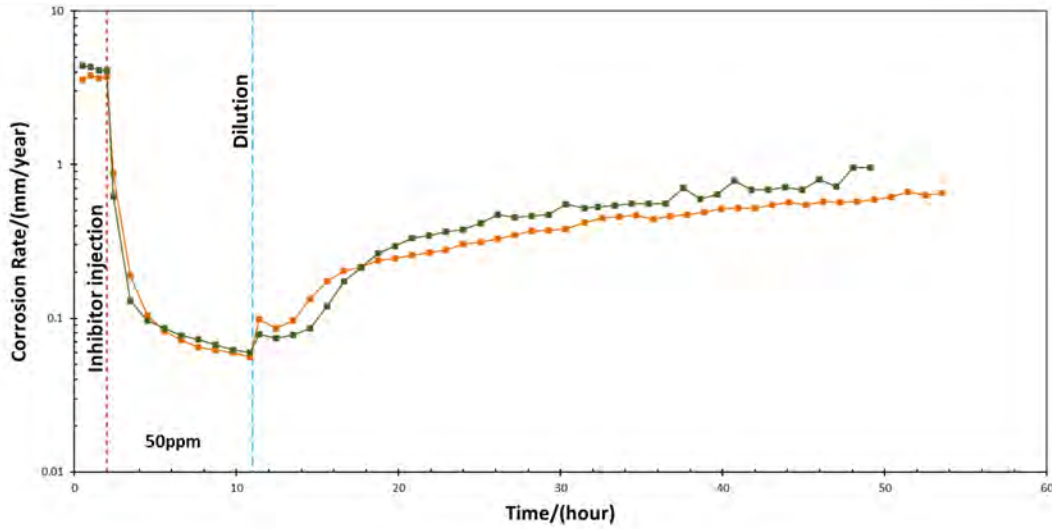


**Figure 7: Corrosion rate versus time for 2 hours pre-corrosion and two different repeats (30°C, 0.97 bar pCO<sub>2</sub>, X65 RCE, 1000 rpm, BDA-C14 inhibitor, 9 hours contact time).**

These results suggest that an increase in the iron carbide at the metal surface could change the surface characteristics and influence the desorption kinetics. Formation of the iron carbide layer decreased the rate of the inhibitor desorption which could enhance the inhibitor persistency.

### **Modeling of desorption behavior using Langmuir isotherm:**

As discussed in the introduction, the Langmuir isotherm model can be used to model inhibitor desorption behavior. This model expresses the change in surface coverage with regards to time as in Equation (4).

$$\frac{d\theta}{dt} = k_A C_{inh}(1 - \theta) - k_D \theta \quad (4)$$

where  $k_A$ ,  $C_{inh}$ ,  $\theta$  and  $k_D$  are adsorption constant ( $M^{-1}.s^{-1}$ ), inhibitor concentration (M), surface coverage factor and desorption constant ( $s^{-1}$ ) respectively. This equation can be solved from two aspects.

#### Adsorption behavior

By solving for surface coverage ( $\theta$ ), and considering  $\theta = 0$  at  $t = 0$ , an explicit function of coverage  $\theta$  with respect to time can be obtained:

$$\theta(t) = \left( \frac{K_{AD} C_{inh}}{1 + K_{AD} C_{inh}} \right) (1 - e^{-(k_A C_{inh} + k_D)t}) \quad (5)$$

where  $K_{AD}$  is equilibrium constant ( $M^{-1}$ ). This equation can be fitted to the experimental data to determine the values of kinetics constants (least squares regression). Figure 8 shows the results of Equation (5) fitted to the experimental data at 30°C. Using this equation fitted to experimental values, adsorption/desorption kinetics constants were calculated and shown in Table 2.

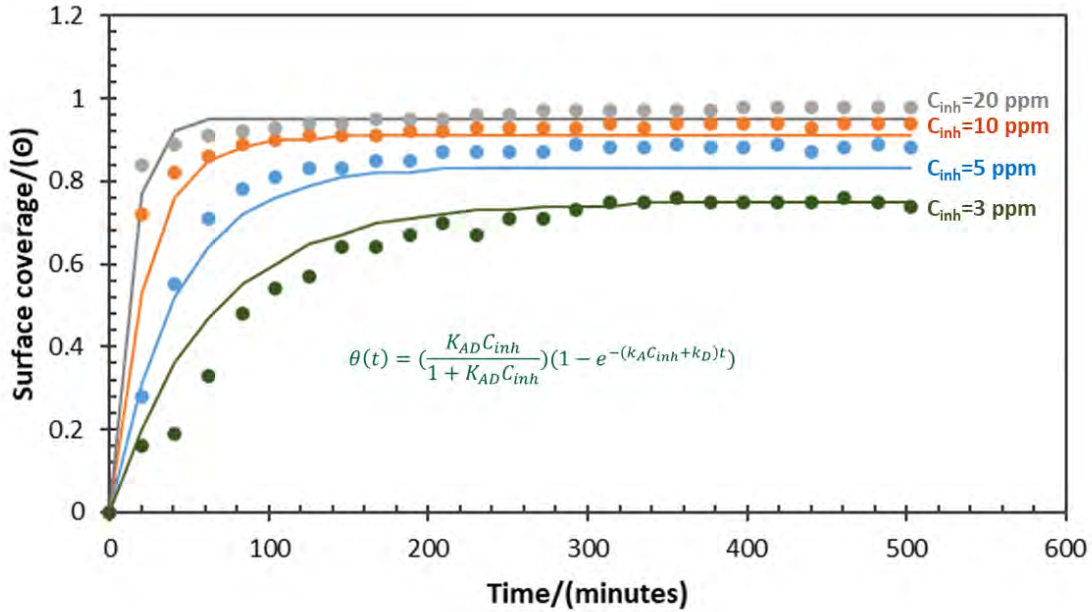


**Figure 8: Langmuir adsorption model fitting with experimental data (30°C, 0.97 bar pCO<sub>2</sub>, X65 RCE, 1000 rpm, BDA-C14 inhibitor).**

**Table 2**  
**Calculated values for adsorption/desorption kinetics at 30°C**

$k_A (mM^{-1} \cdot s^{-1})$	$k_D (s^{-1})$	$K_{AD} (mM^{-1})$
$2.4 \times 10^{-2}$	$6.63 \times 10^{-5}$	371.42

### Desorption behavior

The desorption behavior could be also analyzed using Equation (4). However, this equation requires numerical method to be solved due to the non-constant CI concentration with the time. Thus, at the time of the dilution, by considering  $\theta = 1$  at  $t = 0$  and  $C_{inh}(t) = C_0 e^{(-\frac{Q}{v}t)}$ , the surface coverage can be calculated over time. Then, the corresponding CR can be calculated assuming a direct correlation to coverage using the equation below:

$$CR_{\theta(t)} = CR_{\theta=0} - \theta(t) \times (CR_{\theta=0} - CR_{\theta=1}) \quad (6)$$

where  $CR_{\theta=0}$  is the blank corrosion rate and  $CR_{\theta=1}$  is the stable mitigated corrosion rate with the assumption the inhibitor is fully covering the metal surface. Figure 9 shows the predicted corrosion rate model for the dilution step with 20 minutes pre-corrosion and 9 hours contact time. Figure 10 shows the predicted corrosion rate model compared with the test using a longer contact time but the same 20

minutes pre-corrosion. Figure 11 shows the predicted corrosion rate model compared with the test using a longer pre-corrosion of 29 hours.

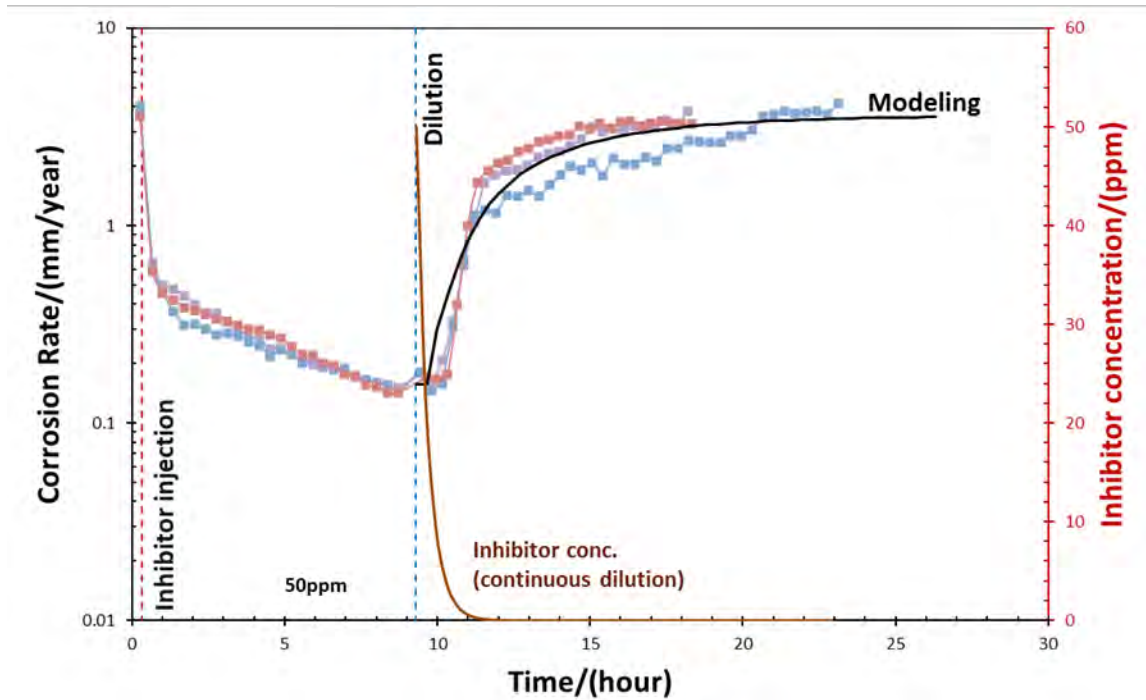


**Figure 9: Modeled corrosion rate versus time compared to experimental data for 20 minutes pre-corrosion and 9 hours contact time (30°C, 0.97 bar pCO<sub>2</sub>, X65 RCE, 1000 rpm, BDA-C14 inhibitor).**

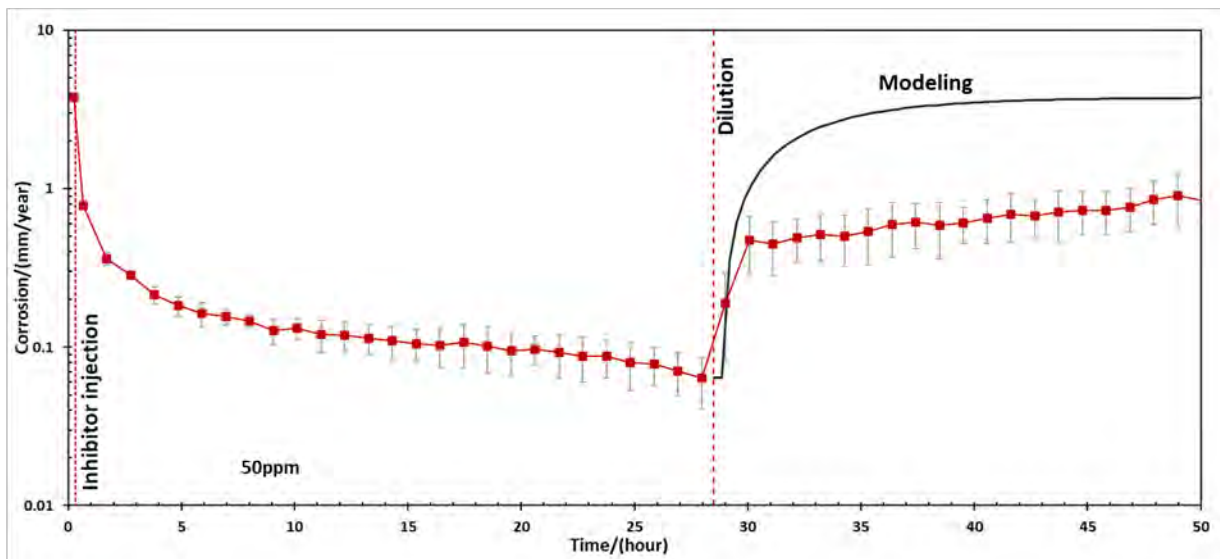


**Figure 10: Modeled corrosion rate versus time compared to experimental data for longer contact time of 29 hours (30°C, 0.97 bar pCO<sub>2</sub>, X65 RCE, 1000 rpm, BDA-C14 inhibitor, 20 minutes pre-corrosion).**

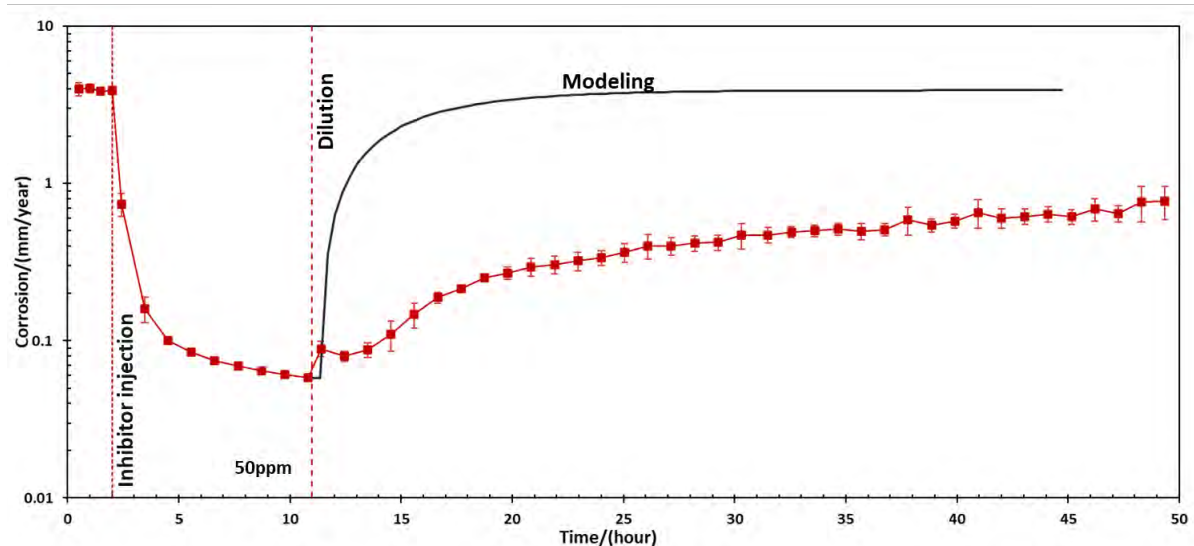


**Figure 11: Modeled corrosion rate versus time compared to experimental data for longer pre-corrosion of 2 hours (30°C, 0.97 bar pCO<sub>2</sub>, X65 RCE, 1000 rpm, BDA-C14 inhibitor, 9 hours contact time).**

Results for the modeling show that the Langmuir isotherm model successfully modeled the desorption behavior of the BDA-C14 on a freshly polished surface. However, the presence of iron carbide residues, associated with longer contact time or pre-corrosion, affected the desorption kinetics as expected. Thus, modeling was not able to predict the desorption behavior of the BDA-C14 when the surface characteristic and corresponding desorption kinetics changed. In addition, the slight delay often observed between the moment the inhibitor dilution starts and the moment the corrosion rate starts to increase may be associated to the time needed for the inhibitor concentration to decrease from 50 ppm to its surface saturation concentration (known to be 20 ppm from other studies)<sup>8</sup>. Thus, inhibitor molecule coverage of the metal surface remained high until the CI concentration in the bulk solution decreased below surface saturation concentration (20 ppm).

## CONCLUSIONS

A new experimental setup was used for mimicking the loss of continuous mitigation treatment of a metal surface by a corrosion inhibitor. Continuous dilution was successfully implemented and was shown to minimize residual corrosion inhibitor content in solution over time. This method for the dilution was used for corrosion inhibitor persistency measurements because it is an easily controlled, very reliable procedure for testing the effects of various parameters (ie. inhibitors contact time, controlled flow rate/fluid exchange rate, longer term studies).

The BDA-C14 model compound inhibitor showed no persistency when all the inhibitor residuals were removed from the bulk. In other words, this model compound inhibitor was shown to follow the adsorption/desorption mechanism which results in no persistency after dilution, similar to other water soluble inhibitors.

Formation of the iron carbide layer on the surface due to longer contact time or longer pre-corrosion time affected the desorption kinetics. This suggests that the iron carbide layer influences inhibitor persistency by decreasing the inhibitor desorption kinetics.

Langmuir isotherm model was shown to be a useful technique for modeling the adsorption and desorption of the inhibitor in continuous inhibition treatment scenarios. Modeling results suggest that continuous treatment inhibition acts in accordance with the adsorption and desorption mechanism which depends strongly on Cl concentration in the bulk but can also be influenced by contact time (ie. length of continuous inhibition time with no failures) and features on the metal surface (ie. iron carbide).

## ACKNOWLEDGEMENTS

The author would like to thank the following companies for their financial support: Ansys, Baker Hughes, Chevron Energy Technology, Clariant Corporation, ConocoPhillips, ExxonMobil, M-I SWACO (Schlumberger), Multi-Chem (Halliburton), Occidental Oil Company, Pertamina, Saudi Aramco, Shell Global Solutions and TotalEnergies. Dr. David Young is thanked for synthesizing the corrosion inhibitor model compounds used in this research with much appreciation given for the technical support from Mr. Alexis Barxias and Mr. Cody Shafer. Dr. Mehdi Rezaei is also thanked for his support in python modeling.

## REFERENCES

1. A. Kahyarian, B. Brown, S. Nestic, "Electrochemistry of CO<sub>2</sub> Corrosion of Mild Steel: Effect of CO<sub>2</sub> on Iron Dissolution Reaction," *Corrosion Science* 129, (2017) pp. 146-151.
2. J. Sonke, W.D. Grimes, "Guidelines for Corrosion Inhibitor Selection for Oil and Gas Production," *CORROSION/2017*, paper no. 8842 (New Orleans, LA: NACE, 2017).
3. S. Webster, D. Harrop, A. J. McMahon, and G. J. Partridge, "A New Class of "Green" Corrosion Inhibitors: Development and Application," *CORROSION/1993*, paper no. 109 (San Antonio, TX: NACE, 1993).
4. M. Lopez, J. Porcayo Calderon, M. Casales Diaz, "Internal Corrosion Solution for Gathering Production Gas Pipelines Involving Palm Oil Amide-based Corrosion Inhibitors," *International Journal of Electrochemical Science* 10, 9 (2015): pp. 7166-7179.
5. P. Roberge, "Corrosion inhibitors" in *Handbook of Corrosion Engineering*, 2<sup>nd</sup> Edition, McGraw-Hill Education, 1995, 833–862.
6. S. Papavinasam, "Mitigation – internal corrosion," in *Corrosion Control in the Oil and Gas Industry*, 1<sup>st</sup> edition, San Diego: Gulf Professional Publishing, 2013, pp. 361-424.
7. S. Papavinasam, "Evaluation and selection of corrosion inhibitors," in *Uhlig's Corrosion Handbook*, Ottawa: John Wiley and Sons, 1999, 1121-1128.
8. M. Pen, K. S. Bahadori, M. Eslami, B. Brown, M. Singer, "Development of Methodologies for Continuous and Batch Inhibitor Film Persistency Investigation in the Laboratory," *CORROSION/2022*, paper no. 18056, (San Antonio, TX: AMPP Annual Conference + Expo, 2022).
9. V.S. Saji, S.A. Umoren, "Corrosion Inhibitors in the Oil and Gas Industry," Weinheim, Germany: John Wiley and Sons, 2020.
10. M. Finšgar and J. Jackson, "Application of Corrosion Inhibitors for Steels in Acidic Media for the Oil and Gas Industry: A Review," *Corrosion Science* 86, (2014) pp. 17-41.
11. S. Papavinasam, *Corrosion Control in the Oil and Gas Industry*, 1st ed. (San Diego, CA: Gulf Professional Publishing, 2013), pp. 361-424.

12. J. A. Dougherty, "Effect of Treatment Method on Corrosion Inhibitor Performance," CORROSION/1997, paper no. 97344 (New Orleans, LA: NACE, 1997).
13. Y. J. Tan, B. Kinsella and S. Bailey, "An investigation of the formation and destruction of corrosion inhibitor films using electrochemical impedance spectroscopy (EIS)," Corrosion Science, 1996, 9, 1545-1561.
14. J. A. Dougherty and B. Oude Alink, "Corrosion and Inhibitor Film life studies using a RCE flow-through test," CORROSION/2002, paper no. 02286, (Denver, CO: NACE 2002).
15. M. Achour, J. Pierce, D. Daniels, "A novel laboratory test method to determine film persistency of batch inhibitors used to mitigate top of the line corrosion," CORROSION/2010, paper no. 10101, (Dallas, TX: NACE 2010).
16. ASTM G185-06 (Reapproved 2020), "Standard Practice for Evaluating and Quantifying Oil Field and Refinery Corrosion Inhibitors Using the Rotating Cylinder Electrode," ASTM International West Conshohocken, PA, 2020.
17. V. S. Sastri, Green Corrosion Inhibitors, 2<sup>nd</sup> edition, New Jersey: John Wiley and Sons, 2011.
18. E. Ituen, O. Akaranta, A. James, "Evaluation of performance of corrosion inhibitors using adsorption isotherm models: an overview," Chemical Sci., vol. 18, no. 1, pp. 1-34, 2017.
19. Y. Liu and L. Shen, "From Langmuir kinetics to first- and second-order rate equations for adsorption," Langmuir, vol. 24, no. 14, pp. 11625-11630, 2008.
20. S. Ramachandran, C. Menendez, Z Liu, "Adsorption and Desorption Analysis of Corrosion Inhibition," CORROSION/2018, paper no. 10805, (Nashville, TN: NACE 2018).
21. R. C. Woollam, R. C. Woollam, "Analysis of Corrosion Inhibitor Performance Curves Using Langmuir Adsorption Kinetics," CORROSION/2021, paper no. 16859, (Salt Lake City, UT: NACE 2021).
22. T. Murakawa, S. Nagaura, and N. Hackerman, "Coverage of iron surface by organic compounds and anions in acid solutions," Corrosion Science, 1967, 7:2, 79-89.
23. M. J. J. Simon-Thomas, Shell Global Solutions, "Corrosion Inhibitor Selection – Feedback from the Field," CORROSION/2000, paper no. 00056 (Orlando, FL: NACE, 2000).